Published in final edited form as:
Hear Res. 2009 September ; 255(1-2): 109–120. doi:10.1016/j.heares.2009.06.006.

Localization and expression of clarin-1, the Clrn1 gene product, in auditory hair cells and photoreceptors

Marisa Zallocchi[a], **Daniel T. Meehan**[a], **Duane Delimont**[a], **Charles Askew**[b], **Suneetha Garrige**[a], **Michael Anne Gratton**[b], **Christie A. Rothermund-Franklin**[c], and **Dominic Cosgrove**[*,a,c]

Marisa Zallocchi: zallocchim@boystown.org; Daniel T. Meehan: meehand@boystown.org; Duane Delimont: delimontd@boystown.org; Charles Askew: ; Suneetha Garrige: garriges@boystown.org; Michael Anne Gratton: mgratton@slu.edu.com; Christie A. Rothermund-Franklin: crothermund-franklin@unmc.edu; Dominic Cosgrove: cosgrove@boystown.org

[a]Boys Town National Research Hospital, 555 North 30th street, Omaha, NE, USA.

[b]University of Pennsylvania, Auditory Research Laboratory, Department of Otorhinolaryngology-HNS, 5 Ravdin ORL, 3400 Spruce St., Philadelphia, PA, USA.

[c]University of Nebraska Medical Center, Omaha, NE, USA.

Abstract

The Usher syndrome 3A (CLRN1) gene encodes clarin-1, which is a member of the tetraspanin family of transmembrane proteins. Although identified more than 6 years ago, little is known about its localization or function in the eye and ear. We developed a polyclonal antibody that react with all clarin-1 isoforms and used it to characterize protein expression in cochlea and retina. In the cochlea, we observe clarin-1expression in the stereocilia of P0 mice, and in synaptic terminals present at the base of the auditory hair cells from E18 to P6. In the retina, clarin-1 localizes to the connecting cilia, inner segment of photoreceptors and to the ribbon synapses. RT-PCR from P0 cochlea and P28 retina show mRNAs encoding only isoforms 2 and 3. Western-blots show that only isoform 2 is present in protein extracts from these same tissues. We examined clarin-1 expression in the immortomouse-derived hair cell line UB/OC-1. Only isoform 2 is expressed in UB/OC-1 at both mRNA and protein levels, suggesting this isoform is biologically relevant to hair cell function. The protein co-localizes with microtubules and post-transgolgi vesicles. The sub-cellular localization of clarin-1 in hair cells and photoreceptors suggests it functions at both the basal and apical poles of neurosensoriepithelia.

Keywords

Usher syndrome; clarin-1; stereocilia; connecting cilia; ribbon synapse

INTRODUCTION

Usher syndrome is the leading genetic disorder of combined blindness and deafness. The main clinical symptoms of the disease are *retinitis pigmentosa* (RP) and hearing loss. Affected

*Correspondence to: Dominic Cosgrove, Ph.D., Director of Basic Research, National Usher Syndrome Center, Boys Town National Research Hospital, 555 No. 30th St., Omaha, NE 68131, Phone: (402) 498-6334, Fax: (402) 498-6331, email: cosgrove@boystown.org.

individuals have a sensorineural hearing impairment at birth and later develop progressive visual impairment secondary to RP. Out of the 20,000 deaf and blind people in the United States, it is estimated that over half have Usher Syndrome. Usher syndrome is clinically and genetically heterogeneous. Three types of Usher Syndrome (I, II, and III) have been identified clinically and are distinguished by severity and progression of hearing loss along with the presence or absence of vestibular dysfunction and the onset of RP. The frequency of Usher has been estimated at 4.4/100,000 in the U.S. (Boughman et al., 1993) and 3.0/100,000 in Scandinavia (Hallgren, 1959).

The genes responsible for 9 of the potentially 11 different forms of Usher syndrome have been identified; 6 of these in the last thirteen years (Adato et al., 2002; Fields et al., 2002; Weil et al., 2003; Ahmed et al., 2001; Bitner-Glindzicz et al., 2000; Bolz et al., 2001; Bork et al., 2001; Eudy et al., 1998; Verpy et al., 2000; Weil et al., 1995; Weston et al., 2004; Ebermann et al., 2007). USH1A and USH2B have recently been discounted as false positive identifications (Gerber et al., 2006, Hmani-Aifa et al., 2009).

Some of the proteins products encoded by the USH genes have been shown to interact with one another in various ways, and may constitute key components of a pathway for developmental and functional maintenance of both hair cells and photoreceptors, with a potential functional connection related to stereociliary development and maintenance (Boeda et al., 2002; Siemens et al., 2002; Weil et al., 2003). With the exception of myosin VIIa and SANS, all the usher proteins are expressed as multiple isoforms (Reviewed in El-Amraoui and Petit, 2005; Kremer et al., 2006). The protein isoforms are often expressed in both tissue specific and sub-cellular compartmentalized manner, adding to the complexity of deciphering the function of the usher proteins (Adato et al., 2005a,b; Reiners et al., 2006; van Wijk et al., 2006). Harmonin is expressed in at least three protein isoforms that are differentially distributed along the length of retinal photoreceptors (Reiners et al., 2003), and within the apical structures of hair cells (Boeda et al., 2002). There are specific exons found in transcripts only expressed in the inner ear, raising the possibility for organ/cell-specific functional domains (Johnson et al., 2003).

Usher syndrome type 3A is caused by mutations in the CLRN1 gene which encodes a protein named clarin-1. While the gene responsible for USH3A was identified more than 6 years ago, protein localization in the cochlea and the retina has never been determined definitively, and the function of clarin-1 remains completely unknown (Joensuu et al., 2001, Fields et al., 2002, Adato et al., 2002, Ebermann et al., 2007). Moreover, there is no evidence of clarin-1 interaction with other usher proteins. Alternative splicing of the mouse Clrn1 gene can result in the potential expression of three distintc protein isoforms: Isoforms 1 (27.9 kDa) and 2 (25.8 kDa), both contain four-transmembrane domains, and isoform 3 (19.2 kDa) that contains only two (Adato et al., 2002). Based on sequence homology, clarin-1 belongs to a large hyperfamily of small integral proteins with four transmembrane domains (TM4SF) that includes two more clarins, tetraspanins, connexins, claudins and calcium channel gamma subunit-like proteins (CACNGS) (Adato et al., 2002, Aarnisalo et al., 2007). Members of this hyperfamily are involved in a variety of processes from cell sorting and signaling to cell-cell interaction and scaffolding functions (Hemler, 2001, Berditchevski, 2001, Adato et al., 2002). A high sequence similarity exists between clarin-1 and a protein called stargazin (CACNG2), a tretraspanin that is involved in regulation of AMPARs targeting and clustering at the cerebellar synapses (Letts et al., 1998, Chen et al., 2000, Tomita et al., 2007, Kato et al., 2008, Payne, 2008). Based on this similarity it has been proposed that clarin-1 may also function at the synapse (Adato et al., 2002).

Here we provide evidence of clarin-1 protein expression in cochlear hair cells and inner segments and synaptic regions of photoreceptors. Isoform 2 is the predominant isoform

expressed in both types of neurosensory cells. In mouse cochlea, clarin-1 is expressed at the apical and basal aspects of the hair cells with a very precise temporal and spatial pattern of expression at the base of the hair cells that parallels afferent synapse maturation. This temporal/spatial expression pattern is a feature also shared by other Usher proteins, suggesting that clarin-1 may be functionally connected to other Usher syndrome proteins.

MATERIALS AND METHODS

Mice

Mice were 129 Sv/J wild type, and bred in house. All experiments using mice were carried out under an approved IACUC protocol, and every effort was made to minimize pain and discomfort related to experimental use of mice

Antibody production and qualification

Antibody production—A fusion peptide construct comprising exons 1 and 4 of mouse clarin-1, common to all three isoforms, was constructed using the PGEX GST bacterial expression construct (Pharmacia, Piscataway, NJ). Protein was collected purified from supernatant following osmotic shock using anti-GST agarose affinity purification according to the methods provided by the manufacturer (Sigma). The antibody was raised in rabbits under contract with Chemicon (Temecula, CA) and IgG was purified from serum using protein A sepharose (Sigma).

Antibody qualification—Cochleae, eyes and UB/OC-1 (University of Bristol/Organ of Corti-1) cells were prepared for immunochemistry as described below. The tissue sections and cells were incubated with anti-clarin-1 antibody or normal rabbit IgG. P3 cochlea sections were also incubated with anti-clarin-1 antibody alone or in the presence of 100-fold molar excess of the fusion protein used to generate the antibody (competitive inhibitor). Antibody specificity was also assessed by western blot analysis of P3 cochlea extracts and UB/OC-1 cells stablily transfected with clarin-1 isoform 2 cloned into pAAV-IRES-hrGFP (Strategene) expression vector with the green fluorescence fusion protein (GFP) at the carboxy-terminus. Blots were probed with anti-clarin-1 antibody or normal rabbit IgG as described below. Anti-clarin-1 antibody specificity was further demonstrated by siRNA knockdown using Ambion's p*Silencer*™ 4.1-CMV plasmid system according to the manufacturer specifications. UB/OC-1 cells were stabily transfected with a siRNA specific for clarin-1 (Sense oligo: GATCCAGAAGGGACCTATGCCTACTTCAAGAGAGTAGGCATAGGTCCCTTCTTTA, Antisense oligo: AGCTTAAAGAAGGGACCTATGCCTACTCTCTTGAAGTAGGCATAGGTCCCTTCTG) or a scrambled siRNA (negative control siRNA) that has no sequence homology with the mouse genome. The knockdown was tested by western-blot, the membrane was cut in half. The upper half (40kDa to 250 kDa) was probed with anti-β-actin antibody as loading control and the lower half (40kDa to 20kDa) was probed with the anti-clarin-1 antibody.

General antibodies

Mouse monoclonal anti-synapsin I antibody (BD Pharmingen, SanDiego CA) was used as an axon terminal marker (Bergeron et al., 2005). Goat-polyclonal anti-centrin-1 antibody (M-15, Santa Cruz Biotechnology) was used to identify the connecting cilium in photoreceptors cells (Trojan et al., 2008) and rabbit polyclonal anti-mannosidase II antibody was a gift from Dr. Marilyn Farquhar (Velasco et al., 1993) and was used to identify the *cis-medial* Golgi subcellular compartment in UB/OC-1 cells. Mouse IgM anti-human β-tubulin antibody was from BD Pharmingen (SanDiego CA). Mouse monoclonal anti-β-actin (Sigma) antibody was used as loading control in siRNAs knockdown assays.

Immunochemistry

Cochlea—Cochleae were obtained from embryonic day 18 (E18) and postnatal day 0–10 (P0–P10) mice. The cochleae were surgically removed, fixed with 4% paraformaldehyde in 0.1M phosphate buffer (pH 7.4) for 4 hours at 4°C and decalcified (P6 and P10) in 0.1 M phosphate buffer (pH 7.4) containing 0.15 M EDTA overnight at 4°C. Cochleae were then mounted in OCT, frozen and cryosectioned at 14 μm thickness. Cross-sections were incubated in a blocking/permeabilizing solution for at least 30 minutes at room temperature (10% non-fat dry milk, 10% glycerol, 0.2% Tween-20 in PBS) and then incubated overnight in blocking solution with the corresponding primary antibody (0.5 μg/ml anti-clarin-1 antibody, 1:300 dilution for synapsin I). After 3 PBS washes, the sections were incubated for 1 hour at room temperature in blocking solution with a 1:600 dilution of the appropriate secondary IgG Alexa-conjugated antibody alone or in combination with Alexa-conjugated phalloidin 1:400 (Invitrogen).

For the dextran labeling experiments a different blocking solution and a higher concentration of anti-clarin-1 antibody were used as there is some protein degradation during the four hours incubation of the cochleae (see Neuronal tracer application section). Briefly, dextran labeled sections were blocked for 30 minutes at room temperature with 0.1 M phosphate buffer containing 0.1% Triton X-100 (Sigma, St. Louis, MO.) and 5% FCS. The incubation with the anti-clarin-1 antibody (5 μg/ml) was done in the same blocking solution overnight at 4°C.

Whole mounts—Organs of Corti were isolated from P0 and P1 cochleae, mounted on BD Cell-Tak (BD Pharmingen SanDiego CA) and fixed with 4% paraformaldehyde in 0.1 M phosphate buffer (pH 7.4) for 30 minutes on ice. Slides were washed with PBS and permeabilized with 0.1% Triton X-100 for 10 minutes on ice, followed by three PBS washes and then immunostained for clarin-1.

Retina—Eyes from adult mice (P28) were microdissected and immediately cryoprotected with 30% sucrose in 0.1 M phosphate buffer for two hours. Eyeballs were then mounted in OCT, frozen and cryosectioned at 12 μm thickness. The sections were fixed with ice cold acetone for 10 minutes, dried for 2 hours and immunostained for clarin-1 (0.5 μg/ml) and centrin-1 (1:50) in PBST 0.1% with 5% FCS.

UB/OC-1 cells—Differentiated UB/OC-1 cells were grown on poly-L-lysine coated microscope slides. Prior to immunostaining, they were rinsed with PBS, fixed with −20°C acetone for 5 minutes and dried for 2 hours at 25°C. Slides were washed once with PBS for 5 minutes, permeabilized with 0.3% Triton X-100 for 10 minutes, followed by three successive PBS washes and then incubated with Image-iT FX signal enhancer (Invitrogen) for 30 minutes in a humidified chamber at 25°C. The slides were washed and blocked with 2% FCS, 0.2% fish gelatin (Sigma) in PBS for 2 hours. The slides were then incubated in blocking solution with 0.5 ng/ml anti-clarin-1 antibody overnight in a humidified chamber at 25°C. After 3 PBS washes, slides were incubated in blocking solution with a 1:1500 dilution of goat anti-rabbit IgG Alexa-555-conjugated 2° antibody (Invitrogen) alone or in combination with 1:2000 dilution of Alexa-488-conjugated phalloidin. Mouse anti human β-tubulin and rabbit anti-mannosidase II antibodies were used at 1:200 and 1:500 dilutions, respectively. Nocadozole, brefeldin A and tyrphostin A8 were purchased from Calbiochem (Gibbstown, NJ). A 10 mM nocodazole stock solution was prepared in DMSO, and added to the medium at a 1:1000 dilution for 15 minutes. Tyrphostin A8 and brefeldin A were dissolved in ethanol and used at 20 μM and 1 μg/ml final concentrations, respectively, for 30 minutes. Drug treatments were done prior to cell fixation and processing for immunohistochemistry.

In all the cases, slides were cover slipped in Vectashield mounting medium with DAPI (Vector, Burlingeme, CA.) and confocal images captured under a Zeiss AxioPlan 2IF MOT microscope interfaced with a LSM510 META confocal imaging system. Final figures were assembled using Adobe Photoshop and Illustrator software (Adobe Systems, San Jose, CA).

Immunoelectron Microscopy

A post-embedding technique was used. Mouse cochleae were microdissected and fixed with 4% paraformaldehyde/0.1% glutaraldehyde in 0.1 M sodium cacodylate buffer (pH 7.4). Cochleae were then rinsed in buffer and embedded in 2% agar, dehydrated in a graded ethanol series (70% at 4°C, 80% at 4°C, 90% at −20°C) and infiltrated (100% + LR White 12hrs at −20°C, then LR White 24hrs −20°C). Samples were bisected and embedded in LR White (Electron Microscopy Sciences, Fort Washington, PA) and cured at −20°C with UV light for 72hrs. Mid-modiolar thin sections (80 nm), mounted on formvar-coated nickel slot grids, were incubated on a blocking buffer containing 1% ovalbumin and 0.1% cold fish gelatin, followed by the clarin-1 primary antibody (1:50) or blocking buffer only (18h, 4°C). After 3 washes in Tris buffer (5 min each), sections were floated on an anti-rabbit IgG conjugated with 10nm colloidal gold (Aurion, Wageningen, Netherlands, 1:20, 1 h, 23°C), followed by 2 washes each in Tris buffer and deionized water. Sections were viewed on a JEOL 1010x transmission electron microscope where digitized images were acquired and archived an Orca CCD camera (Hamamatsu Photonics, Bridgewater, NJ) and AMT Advantage 12-HR software (version 5.4.2.239, Advanced Microscopy Techniques, Danvers, MA).

Neuronal tracer application

Cochleae from P3 mice were microdissected and used for neuronal tracer labeling of the type I afferent fibers as described by Boyer et al., 2004 and Huang et al., 2007. Briefly, P3 mice were killed, heads sectioned in the sagital plane and the brain removed. Dye conjugated dextran was applied to the freshly cut vestibulocochlear nerve and incubated at room temperature for 20 minutes. Cochleae were microdissected and incubated for 4 h at room temperature in aerated artifical cerebrospinal fluid, aCSF (130 mM NaCl, 3 mM KCl, 2 mM $CaCl_2$, 1.3 mM NaH_2PO_4, 2 mM $MgSO_4$, 20 mM glucose, 20 mM $NaHCO_3$, 0.4 mM ascorbic acid, pH 7.4). After fixation by immersion in 4% paraformaldehyde in PBS, the tissue was mounted in OCT, cryosectioned at 14 μm, and processed for confocal microscopy.

Western blot

For total eye and cochlea, P28 and P0 wild type mice were used respectively. The tissue was homogenized in RIPA buffer in the presence of protease inhibitors (Sigma P8340) and the homogenate was cleared by centrifugation at 10,000 rpm for 10 min at 4°C. Differentiated UB/OC-1 cells were harvested in RIPA buffer with protease inhibitors prior 3 rinses with cold PBS and the cell lysate was cleared by centrifugation at 10,000 rpm for 10 min at 4°C. Protein concentration was measured using the Bio-Rad assay protocol (500-0006).

Twenty micrograms of protein for eye and UB/OC-1 cells and 40 μg for cochlea were resolved in a 10% SDS-PAGE, under reducing conditions, transferred to PVDF membranes for 1 hour using 100 V at 4°C and blocked overnight at 4°C with rocking in 10% non-fat dry milk containing 0.1% Tween 20. The rabbit anti-mouse clarin-1 antibody was diluted to 2 ug/ml in 10% milk blocking solution and incubated overnight at 4°C. After two washes the secondary antibody (anti-rabbit HRP-conjugated, Sigma A9169) was diluted 1/20,000 in milk blocking solution and incubated for 1 hour at room temperature. The protein bands were revealed using the ECL system (Pierce 32106).

RT-PCR

RT-PCR was carried out on RNA from P0 cochlea, P28 neuroretina and differentiated UB/OC-1 cells. Primers were designed to comprise the entire coding sequence of Clrn1 gene (forward primer: ATGCCAAGCCAGCAGAAG; reverse primer: GTACATTAAATCTGAAGCTACATTAGTGG). Four micrograms of total RNA was reverse transcribed using the Superscript reverse transcriptase kit (Invitrogen). One tenth of the synthesized cDNA was used for PCR in a total volume of 50 μL using 0.4mM of primers and Platinum PCR Supermix (Invitrogen). After denaturation, the transcripts were amplified by 35 cycles of 94°C/60°C/72°C for 30 sec/30sec/60sec respectively. PCR products were resolved by agarose gel electrophoresis on 2.0% gels.

Cell Culture

Cultivation of UB/OC-1, a conditionally immortal auditory hair cell line, was conducted as previously reported (Rivolta et al., 1998) with noted exceptions. In brief, UB/OC-1 cells were maintained in DMEM/F-12 medium (Invitrogen, Grand Island, New York) supplemented with 5% fetal bovine serum (FBS; Atlanta Biologicals, Lawrenceville, GA), 100U/ml penicillin, 0.1 mg/ml streptomycin and 0.29 mg/ml L-glutamine (Invitrogen). To propagate UB/OC-1 cells were maintained at 33° C and the culture medium supplemented with 10 U/ml mouse recombinant γ-interferon (Calbiochem, La Jolla, CA.). Subconfluent cultures were dissociated with 0.05% trypsin,0.02% EDTA (Invitrogen) and re-plated at 1:5. To induce differentiation, dissociated cells were plated in medium without γ-interferon, allowed to attach overnight at 33°C and then maintained at 39° C without γ-interferon for at least 10 days.

Differentiated UB/OC-1 cells were dissociated, plated onto poly-L-lysine coated microscope slides (VWR, Batavia, IL) pretreated with 5% FBS containing medium and maintained at 39° C for at least 3 days. Slides were subsequently treated with nocodazole 10 mM, brefeldin A 1 μg/μl or tyrphostin A8 20 μM and analyzed by confocal microscopy.

RESULTS

Immunolocalization of clarin-1 in mouse cochlea and retina

The intron/exon structure of the mouse Clrn1 gene is shown in Figure 1, along with the alternative splice variants expected in the clarin-1 proteins. Exons 1 and 4 were expressed as a recombinant protein and used to raise an anti-clarin-1 antibody. This antibody was designed to recognize all isoforms of clarin-1, as the three isoforms share the first and last exons (Adato et al. 2002).

The specificity of the clarin-1 antibody was determined by multiple approaches (Figure 2). Figure 2I shows confocal microscopy studies of mid-modiolar P3 cochlea sections, P28 retina and UB/OC-1cells immunostained with anti-clarin-1 antibody or pre-immune rabbit IgG. Only sections incubated with the anti-clarin-1 antibody show specific immunostaining. Figure 2III shows competitive inhibition for clarin-1 immunostaining by inclusion of 100-fold molar excess of peptide immunogen in the incubation buffer. Western-blot analysis of P3 cochlea extracts (Figure 2II) shows a band of the correct molecular size when the membrane was probed with anti-clarin-1 antibody (lane 1, arrowhead) but not when probed with pre-immune rabbit IgG (lane 2). Extracts from UB/OC-1 cells stablily transfected with GFP-clarin-1 revealed two bands corresponding to the endogenous clarin-1 (lane 3, arrowhead) and the GFP-fusion protein (lane 3, asterisk). Finally, Figure 2IV show the knockdown of clarin-1 in UB/OC-1 cells by siRNA technology. Cells expressing a siRNA specific for clarin-1 showed a marked decrease in protein expression compared to cells transfected with a control siRNA (scrambled siRNA). Collectively, these data clearly establish the specificity of the Clarin-1 antibody preparation used in this study. Potential cross reactivity with Clarin-2 and Clarin-3 is unlikely,

given that they do not contain enough continuous amino acid sequence identity to constitute an epitope (maximum of 5).

Clarin-1 immunostaining and confocal microscopy was used to explore the subcellular distribution of clarin-1 in mouse cochleae from E18 to P10. At E18 clarin-1 is already present in the organ of Corti at the base of both the inner and outer hair cells, with robust staining around the basal aspects of the inner hair cells (Figure 3A–C). This signal at the basal aspect of the hair cells persists from P0 (Figure 3D–F) to P6 (Figure 3G–L) with some immunostaining in the cell body of outer hair cells. By P10, clarin-1 is no longer observed at the base of the outer hair cells, but a weak immunostaining persists at the base of the inner hair cells. At the apical aspect of the hair cells, we detected localization of clarin-1 to the stereocilia in P0 mouse cochleae (Figure 3D–F and Figure 4A–C). Interestingly, by P1, clarin-1 is no longer observed in the stereocilia although a weak intracellular immunostaining is still detectable (Figure 4D–F, asterisk). Immunogold labeling confirms localization of clarin-1 to the stereocilia in P0 mice (Figure 4G). Together, these results suggest developmental regulation of clarin-1 expression in mouse cochleae. The regulation at the base of outer hair cells (OHCs) is distinct from that at the apical aspect of the OHCs, suggesting that regulated transport and/or turnover of clarin-1 may play a role in its developmental expression.

Retinal pathology in Usher syndrome type III patients is delayed onset, initiating during adolescence or early adulthood. We therefore studied clarin-1 distribution in the adult mouse as a more clinically relevant developmental stage. In the adult mouse photoreceptors clarin-1 is expressed at the ribbon synapses, inner segments and connecting cilia (Figure 5A–C). We also observed a strong immunostaining for clarin-1 at the base of the connecting cilium shown by partial colocalization with centrin-1 (Figure 5D–F).

Since the almost identical spatiotemporal expression pattern of clarin-1 (Figure 3) and type I neuron afferent to efferent synaptic maturation in the cochlea (Pujol 1985;Sobkowitz et al., 1982;Pujol et al., 1998;Huang et al., 2007) we decided to investigate whether clarin-1 is present at the synaptic terminals of type I afferent neurons in P3 cochleae. Figure 6I shows colocalization of clarin-1 with synpasin I (a marker for axonal terminals) below the OHCs and inner hair cell (IHC). However, while synapsin I is extensively expressed along the axonal fiber, clarin-1 has a more restricted expression with an almost exclusive localization below the hair cells. Using a technique developed by Boyer et al., 2004 and adapted by Huang et al., 2007, in which type I afferent terminals can be specifically labeled by a fluorochromo-conjugated dextran, we were able to identify the source of dendrites that are immunopositive for clarin-1. As shown in Figure 6II (panels A–C), there is a partial overlap between the type I afferent dextran-labeled terminals and clarin-1 immunostaining, suggesting that clarin-1 is present in type I afferent synapses in P3 cochleae but also at the basal aspect of the OHCs which were not labeled by the dextran (asterisk in inset), indicating both pre- and post-synaptic localization. Figure 6II (panels D–F), show a dual staining with phalloidin to demosntrate the integrity of the organ of Corti after the 4 hours incubation needed for the dextran to diffuse to the synaptic terminals.

Isoform specificity and UB/OC-1 subcellular localization of clarin-1

As noted in figure 1, differential mRNA splicing can result in the potential expression of three different clarin-1 protein isoforms. To characterize which of these isoforms are expressed in cochlea and retina we designed PCR primers flanking the 5’ and 3’ terminal translated portion of the clarin-1 mRNA. These primers were used to amplify mouse cDNA from P0 cochleae and P28 retinas. In addition, we utilized a conditionally immortalized hair cell line from E-16 murine organ of Corti (the UB/OC-1 cell line originally developed in Mathew Holly’s laboratory [Rivolta et al., 1998,2002]), to characterize clarin-1 mRNA expression in cochlear hair cells. Differentiated cells were used to prepare RNA for RT-PCR analysis, since

differentiation was previously shown to elevate Myosin VIIa mRNA expression in these cells (Rivolta et al., 2002), an observation we found also to be true for clarin-1 mRNA expression (data not shown). The results in Figure 7A show that two transcripts are detected in RNA from cochlea and retina that correspond to the predicted sizes of the 232 amino acid (696 bp) and the 172 amino acid (516 bp) isoforms (isoforms 2 and 3, Figure 1) of clarin-1, confirmed by sequence analysis. In contrast, only the 696 bp transcript (isoform 2) is observed in mRNA isolated from UB/OC-1 cells. The transcript encoding the 250 amino acid isoform of clarin-1 (PCR product size of 752 bp) was not observed. Western blot analysis was performed on extracts of P0 cochleae and P28 eyes from mice as well as extracts of UB/OC-1 cells. The results in Figure 7B show a single clarin-1 isoform is predominantly expressed at the protein level with an apparent molecular mass of 30 kDa. This isoform is most likely isoform 2 (predicted size 25.8 kDa), since this is the only transcript expressed in OC-1 cells. Differences in observed *versus* predicted molecular mass could be due to either electrophoretic conditions or to post-translational modifications. Western blot analysis was negative when the protein lysates were probed with an affinity purified IgG from pre-immune rabbits (Figure 2II).

Immunostaining of UB/OC-1 cells with anti-clarin-1 antibody shows a filamentous cellular localization with a concentration of immunostaining surrounding the nucleus (Figures 8A and 8D). Cells were counterstained with phalloidin to determine whether clarin-1 co-localized with actin filaments. Figure 8B and C show distinct non-overlapping staining for clarin-1 and phalloidin indicating that clarin-1 does not co-localize with actin. Immunostaining using affinity purified IgG from pre-immune rabbits did not show positive immunofluorescent signal (Figure 2I). Dual immunostaining of UB/OC-1 cells with tubulin (panel E) and clarin-1 (panel D) shows complete colocalization (panel F) suggesting clarin-1 may be associated specifically with microtubules in these cells. To determine whether this is indeed the case, we treated cells for 15 minutes with nocodozole, which inhibits tubulin polymerization (Head et al., 2006). Under these conditions, both clarin-1 (panel G) and tubulin (panel H) show a loss of filamentous localization, indicating that clarin-1 is directly associated with the microtubules (panel I).

We also tested the effect of two drugs that influence trafficking of different types of vesicles in UB/OC-1 cells. Tyrphostin A8, affects post-transGolgi vesicle transport by blocking a specific subset of small monomeric GTPases (Lütcke et al., 1993) and brefeldin A, which inhibits COPI vesicles trafficking form the Golgi back to the ER producing a dispersion of the cis-Golgi proteins (Beller et al., 2008, Duijsings et al., 2009).

Treatment of differentiated UB/OC-1 cells with tyrphostin A8 resulted in dispersion of the co-localization of clarin-1 with the microtubules (Figure 8J and 8L) while leaving the microtubules intact (Figure 8K). In contrast, brefeldin A had no effect on clarin-1 filamentous distribution as shown by Figure 9A–B. Mannosidase II, a marker for the *cis-medial* Golgi compartment, was dispersed in response to brefeldin A treatment (Figure 9C–D) confirming the specificity of the drug. These results suggest that clarin-1 is present in post-transGolgi vesicles associated to the microtubule cytoskeleton in UB/OC-1 cells.

DISCUSSION

The association of clarin-1 with Usher syndrome type 3A was described in 2002 (Adato et al., 2002; Fields et al., 2002). Since then, almost nothing has been described regarding the expression and/or possible function of clarin-1 in inner ear and photoreceptors cells. Here, we show for the first time the pattern of expression of clarin-1 in these two specialized neuroepithelia at the protein level.

Our results indicate that clarin-1 has a very specific pattern of expression in mouse cochleae. It is developmentally expressed from E-18 (the earliest age we looked at,) to P10, a feature

that is also share by other Usher proteins (El-Amraoui and Petit, 2005). At the apical aspect of the hair cells clarin-1 was only detected at P0 by both dual confocal immunostaining with phalloidin and by transmission electron microscopy. This narrow window of expression in the stereocilia is surprising, but highly reproducible, and was observed using both whole mount and mid-modiolar cross sections of the cochlea. This finding suggests that clarin-1 protein has a distinct developmental expression window at the basal region of the hair cell *versus* the apical region, which implies distinct windows for clarin-1 function at the two poles.

The tempospatial pattern of expression at the base of the hair cells overlaps with the developmental neuronal switch that occurs postnatally in mouse OHCs, during which time afferent type I synaptic terminals are replaced by the efferent synaptic terminals that persist to adulthood (Pujol, 1985; Sobkowitz et al., 1982; Pujol et al., 1998; Huang et al., 2007). This suggests that clarin-1 may be involved in synaptic maturation. As a first step towards the elucidation of the type of cells that expressed clarin-1 during this developmental window, we double immunostained midmodiolar sections from P3 mouse cochleae with anti-clarin-1 and anti-synapsin I antibodies. We observed colocalization of both proteins below the hair cells confirming the neuronal nature of the cells expressing clarin-1. However, clarin-1 expression was confined to the very end of the neuronal terminals, with absence of clarin-1 immunostaining along the neuronal fibers that were still positive for synapsin I.

By dextran labeling we were able to determine the nature of the synaptic terminals that expressed clarin-1. This technique was originally developed by Boyer et al., 2004 and modified by Huang et al., 2007, and permits the specific labeling of afferent type I terminals by a fluorochromo conjugated dextran. Cross-sections of P3 mouse cochleae treated this way and immunostained for clarin-1 show partial colocalization of clarin-1 with the dextran confirming not only its expression in type I afferent terminals but also a pre-synaptic expression at the base of the OHCs.

Developmental studies of other Usher proteins in mouse cochleae suggest that one function for these proteins is to participate in developmentally regulated cohesive complex formation that regulates appropriate development of stereocilia (El-Amraoui and Petit, 2005; Lefevre et al., 2008). Expression of clarin-1 at the stereocilia at P0 suggests it may play a role in stereocilia development as well. While myosin VIIa is always present in stereocilia, whirlin, VLGR1b, and usherin are expressed transiently (El-Amraoui and Petit, 2005; Michalski et al., 2007; McGee et al., 2006). Thus it will be of interest to determine whether clarin-1 interacts with any of these other usher proteins.

In the retina, we observed expression of clarin-1 at the ribbon synapses and in the inner segments of photoreceptor cells with concentrated immunostaining at the base of the connecting cilium, demonstrating an almost identical subcellular distribution with several other Usher proteins (Reiners et al., 2006).

Recently, a model was proposed based on known protein interactions, immunolocalization, and ultrastructural localization studies that predicts a potential role for the usher protein complex as a part of a periciliary scaffold involved in molecular transport of vesicular cargo between the inner and outer segments of photoreceptors (Maerker et al., 2008). While hypothetical, this model is intriguing with respect to our immunolocalization studies, which show presence of clarin-1 at the base of the connecting cilium of photoreceptors. As proposed, this hypothetical complex would be comprised of the long isoform of usherin, the full length isoform of VLGR1, whirlin, vezatin, and SANS, which is very similar to the proposed complex at the ankle links of developing stereocilia in the mouse (Michalski et al., 2007). It is therefore of interest to see if clarin-1 interacts with any of these proteins, which might suggest a role for

clarin-1 in these similar subcellular compartments of photoreceptors (periciliary region) and hair cells (stereocilia).

Interestingly, expression was detected in the synaptic regions of both sensory cells consistent with observations for other Usher proteins (van Wijk et al., 2006, Kremer et al., 2006). Photoreceptors and hair cells possess ribbon synapses, a specialized type of synapse present in very few neurons (photoreceptors, hair cells, bipolar cells, pinealocytes) (Sterling and Matthews, 2005), where synaptic vesicles are organized along an electron dense structure called ribbon. In the outer hair cells, transient ribbon synapses form between the hair cells and the type I afferent nerve terminals. These persist to around P10 when the ribbons are lost and replaced by large efferent synapses (Sobkowitz et al., 1982, Raphael and Altschuler, 2003). Outer hair cells' ribbons persist to adulthood only at the apex, where they are not prevalent (Moser et al., 2006; Roux et al., 2006). Recently, the transient ribbon synapses have been shown to undergo efficient calcium-dependent neurotransmitter release, demonstrating that they are indeed functional ribbon synapses (Beurg et al., 2008). Coincident expression of clarin- 1 in both the pre and post-synaptic regions of outer hair cell type I afferent ribbon synapses begs the question whether clarin-1 is playing a role in OHC synaptic maturation. This question could be addressed through the development and characterization of an USH3A mouse model.

Usher syndrome is a disease of two unique ciliated neurosensoriepithelial cell types, yet a common cellular pathway that explains syndromic pathobiology has not been identified. This may be due, in part, to the relative absence of a discernable retinitis pigmentosa phenotype in the usher syndrome mouse models, which has stifled progress in understanding retinal pathology associated with Usher syndrome. All of the usher proteins appear to localize to the ribbon synapse and the inner segments and connecting cilia (Reiners et al., 2006; Maerker et al., 2008), while at least two (myosin VIIa and the basement membrane associated isoform of usherin) are expressed in the retinal pigment epithelium (RPE) as well (Liu et al., 1999, Bhattacharya et al., 2004, Bhattacharya and Cosgrove, 2005). Myosin VIIa null mice show defects in phagosome digestion and melanosome motility in the RPE, and in transport of rhodopsin in the connecting cilia of photoreceptors (Liu et al., 1999; Gibbs et al., 2003). All three defects are rescued when myosin VIIa is transfected into the retinal pigment epithelium using lentivirus (Hashimoto et al., 2007). These studies suggest that retinal dysfunction in USH1B patients might also involved functional defects in the retinal pigment epithelium.

There are three putative alternatively spliced transcripts for clarin-1, but only the two smaller transcripts are detected in RNA from either retina or cochlea (confirmed by sequencing). In addition to mouse cochlea and retina, we utilized the conditionally immortalized cochlear hair cell line, UB/OC-1, as an alternative and simpler model system to study clarin-1 expression and subcellular localization in hair cells. We only observed expression of the middle transcript (696 bp) of clarin-1 in differentiated UB/OC-1. Interestingly, only the 232 amino acid isoform of clarin-1 protein is present in extracts from retina, cochlea, or UB/OC-1 cells, suggesting that this is the predominant functional isoform in sensorineural epithelial cells.

Co-localization of clarin-1 to microtubules in UB/OC-1 cells and its possible association to post-transgolgi vesicles was somewhat surprising, as we expected an association with actin microfilaments based on the presence of myosin VIIa in the Usher complex. Given that myosin VIIa, the USH1B gene product, is an unconventional myosin motor that may be involved in actin based protein transport, one may expect other usher syndrome related proteins would be linked to or transported along actin microfilaments. Our data from UB/OC-1 cells may reflect protein packaged in vesicles being actively transported through the cells along microtubules, which are known to serve as scaffold for vesicle trafficking (Neco et al., 2003).

In summary, here, we demonstrated for the first time the expression of clarin-1 at the protein level in the developing inner ear and in the retina. The colocalization of clarin-1 with microtubules and its dispersion upon treatment with post-transgolgi transport inhibitors clearly demonstrated the association of clarin-1 with sorting vesicles, suggesting a potential function for clarin-1 involving vesicle transport and stereocilia/synaptic development and/or maintenance.

ACKNOWLEDGEMENTS

Supported by R01 DC004844 (to DC) and R01 DC 006442 (to MAG). The authors gratefully acknowledge Skip Kennedy for expert preparation of figures, Mathew Holley and Dr. Marilyn Farquhar for the kind gift of UB/OC-1 cells and the mannosidase II antibodies, respectively. Confocal microscopy was conducted at the Integrative Biological Imaging Facility at Creighton University, Omaha, NE. This facility was constructed with support from C06 Grant RR17417-01 from the NCRR, NIH.

REFERENCES

Aarnisalo AA, Pietola L, Joensuu J, Isosomppi J, Aarnisalo P, Dinculescu A, Lewin AS, Flannery J, Hauswirth WW, Sankila EM, Jero J. Anti-clarin-1 AAV-delivered ribozyme induced apoptosis in the mouse cochlea. Hear. Res 2007;230(1–2):9–16. [PubMed: 17493778]

Adato A, Lefevre G, Delprat B, Michel V, Michalski N, Chardenoux S, Weil D, El-Amraoui A, Petit C. Usherin, the defective protein in Usher syndrome type IIA, is likely to be a component of interstereocilia ankle links in the inner ear sensory cells. Hum. Mol. Genet 2005a;14:3921–3932. [PubMed: 16301217]

Adato A, Michel V, Kikkawa Y, Reiners J, Alagramam KN, Weil D, Yonekawa H, Wolfrum U, El-Amraoui A, Petit C. Interactions in the network of Usher syndrome type 1 proteins. Hum. Mol. Genet 2005b;14:347–356. [PubMed: 15590703]

Adato A, Vreugde S, Joensuu T, Avidan N, Hamalainen R, Belenkiy O, Olender T, Bonne-Tamir B, Ben-Asher E, Espinos C, Millán JM, Lehesjoki AE, Flannery JG, Avraham KB, Pietrokovski S, Sankila EM, Beckmann JS, Lancet D. CLRN1A transcripts encode clarin-1, a four-transmembrane-domain protein with a possible role in sensory synapses. Eur. J. Hum. Genet 2002;10339–335

Ahmed ZM, Riazuddin S, Bernstein SL, Ahmed Z, Khan S, Griffith AJ, Morell RJ, Friedman TB, Riazuddin S, Wilcox ER. Mutations of the protocadherin gene PCDH15 cause Usher syndrome type 1F. Am. J. Hum. Genet 2001;69:5–34.

Beller M, Sztalryd C, Southall N, Bell M, Jäckle H, Auld DS, Oliver B. COPI complex is a regulator of lipid homeostasis. PLoS Biol 2008;6(11):2530–2594.

Berditchevski F. Complexes of tetraspanins with integrins: more than meets the eye. J. Cell Sci 2001;114 (Pt 23)

Bergeron AL, Schrader A, Yang D, Osman AA, Simmons DD. The final stage of cholinergic differentiation occurs below inner hair cells during development of the rodent cochlea. J. Assoc. Res. Otolaryngol 2005;6(4):4143–4151.

Beurg M, Safieddine S, Roux I, Bouleau Y, Petit C, Dulon D. Calcium- and otoferlin-dependent exocytosis by immature outer hair cells. J. Neurosci 2008;28(8):1798–1803. [PubMed: 18287496]

Bhattacharya G, Cosgrove D. Evidence for functional importance of usherin/fibronectin interactions in retinal basement membranes. Biochemistry 2005;44(34):11518–11524. [PubMed: 16114888]

Bhattacharya G, Kalluri R, Orten DJ, Kimberling WJ, Cosgrove D. A domain-specific usherin/collagen IV interaction may be required for stable integration into the basement membrane superstructure. J.Cell. Sci 2004;117(Pt 2):233–242. [PubMed: 14676276]

Bitner-Glindzicz M, Lindley KJ, Rutland P, Blaydon D, Smith VV, Milla PJ, Hussain K, Furth-Lavi J, Cosgrove KE, Shepherd RM, Barnes PD, O'Brien RE, Farndon PA, Sowden J, Liu XZ, Scanlan MJ, Malcolm S, Dunne MJ, Aynsley-Green A, Glaser B. A recessive contiguous gene deletion causing infantile hyperinsulinism, enteropathy and deafness identifies the Usher type 1C gene. Nat. Genet 2000;26(1):56–60. [PubMed: 10973248]

Boëda B, El-Amraoui A, Bahloul A, Goodyear R, Daviet L, Blanchard S, Perfettini I, Fath KR, Shorte S, Reiners J, Houdusse A, Legrain P, Wolfrum U, Richardson G, Petit C. Myosin Vlla, harmonin

and cadherin 23, three Usher l gene products that cooperate to shape the sensory hair cell bundle. EMBO J 2002;24:6689–6699.

Bolz H, von Brederlow B, Ramírez A, Bryda EC, Kutsche K, Nothwang HG, Seeliger M, del C-Salcedó Cabrera M, Vila MC, Molina OP, Gal A, Kubisch C. Mutation of CDH23, encoding a new member of the cadherin gene family, causes Usher syndrome type 1D. Nat. Genet 2001;27:108–112. [PubMed: 11138009]

Bork JM, Peters LM, Riazuddin S, Bernstein SL, Ahmed ZM, Ness SL, Polomeno R, Ramesh A, Schloss M, Srisailpathy CR, Wayne S, Bellman S, Desmukh D, Ahmed Z, Khan SN, Kaloustian VM, Li XC, Lalwani A, Riazuddin S, Bitner-Glindzicz M, Nance WE, Liu XZ, Wistow G, Smith RJ, Griffith AJ, Wilcox ER, Friedman TB, Morell RJ. Usher syndrome 1D and nonsyndromic autosomal recessive deafness DFNB12 are caused by allelic mutations of the novel cadherin-like gene CDH23. Am. J. Hum. Genet 2001;68:26–37. [PubMed: 11090341]

Boughman JA, Vernon M, Shaver KA. Usher syndrome: Definition and estimate of prevalence from two high risk populations. J. Chron. Dis 1993;36:595–603. [PubMed: 6885960]

Boyer S, Ruel J, Puel JL, Chabbert C. A procedure to label inner ear afferent nerve endings for calcium imaging. Brain Res. Protoc 2004;13(2):91–98.

Chen L, Chetkovich DM, Petralia RS, Sweeney NT, Kawasaki Y, Wenthold RJ, Bredt DS, Nicoll RA. Stargazin regulates synaptic targeting of AMPA receptors by two distinct mechanisms. Nature 2000;408(6815):936–943. [PubMed: 11140673]

Duijsings D, Lanke KH, van Dooren SH, van Dommelen MM, Wetzels R, de Mattia F, Wessels E, van Kuppeveld FJ. Differential membrane association properties and regulation of class I and class II Arfs. Traffic 2009;10(3):316–323. [PubMed: 19170981]

Ebermann I, School HP, Charbel IP, Becirovic E, Lamprecht J, Jurklies B, Millan JM, Aller E, Mitter D, Bolz H. A novel gene for Usher syndrome type 2: Mutations in the long isoform of whirlin are associated with retinitis pigmentosa and sensorineural hearing loss. Hum. Genet 2007;121(2):203–211. [PubMed: 17171570]

El-Amraoui A, Petit C. Usher I syndrome: unravelling the mechanisms that underlie the cohesion of the growing hair bundle in inner ear sensory cells. J. Cell Sci 2005;118:4593–4603. [PubMed: 16219682]

Eudy JD, Weston MD, Yao S, Hoover DM, Rehm HL, Ma-Edmonds M, Yan D, Ahmad I, Cheng JJ, Ayuso C, Cremers C, Davenport S, Moller C, Talmadge CB, Beisel KW, Tamayo M, Morton CC, Swaroop A, Kimberling WJ, Sumegi J. Mutation of a gene encoding a protein with extracellular matrix motifs in Usher syndrome type lla. Science 1998;280:1753–1757. [PubMed: 9624053]

Fields RR, Zhou G, Huang D, Davis JR, Moller C, Jacobson SG, Kimberling WJ, Sumegi J. Usher syndrome type III: Revised genomic structure of the CLRN1 gene and identification of novel mutations. Am. J. Hum. Genet 2002;71:607–617. [PubMed: 12145752]

Gerber S, Bonneau D, Gilbert B, Munnich A, Dufier JL, Rozet JM, Kaplan J. USH1A: Chronicle of a slow death. Am. J. Hum. Genet 2006;78:327–359.

Gibbs D, Kitamoto J, Williams DS. Abnormal phagocytosis by retinal pigmented epithelium that lacks myosin VIIa, the Usher syndrome 1B protein. Proc. Natl. Acad. Sci. U. S. A 2003;100:6481–6486. [PubMed: 12743369]

Hallgren B. *Retinitis pigmentosa* combined with congenital deafness; with vestibulo-cerebellar ataxia and neural abnormality in a proportion of cases. Acta Psychiatr. Scand. Suppl 1959;135:1–100.

Hashimoto T, Gibbs D, Lillo C, Azarian SM, Legacki E, Zhang XM, Yang XJ, Williams DS. Lentiviral gene replacement therapy of retinas in a mouse model for Usher syndrome type 1B. Gene Ther 2007;14:584–594. [PubMed: 17268537]

Head BP, Patel HH, Roth DM, Murray F, Swaney JS, Niesman IR, Farquhar MG, Insel PA. Microtubules and actin microfilaments regulate lipid raft/caveolae localization of adenylyl cyclase signaling components. J. Biol. Chem 2006;281(36):26391–26399. [PubMed: 16818493]

Hemler ME. Specific tetraspanin functions. J. Cell. Biol 2001;155(7)

Hmani-Aifa M, Benzina Z, Zulfiqar F, Dhouib H, Shahzadi A, Ghorbel A, Rebai A, Soderkvist P, Riazuddin S, Kimberling WJ, Ayadi H. Identification of two new mutations in the GPR98 and the PDE6B genes segregating in a Tunisian family. Eur. J. Hum. Genet 2009;17(4):474–482. [PubMed: 18854872]

Huang LC, Thorne PR, Housley GD, Montgomery JM. Spatiotemporal definition of neurite outgrowth, refinement and retraction in the developing mouse cochlea. Development 2007;134(16):2625–2933.

Joensuu T, Hämäläinen R, Yuan B, Johnson C, Tegelberg S, Gasparini P, Zelante L, Pirvola U, Pakarinen L, Lehesjoki AE, de la Chapelle A, Sankila EM. Mutations in a novel gene with transmembrane domains underlie Usher syndrome type 3. Am. J. Hum. Genet 2001;69(4):673–684. [PubMed: 11524702]

Johnson KR, Gagnon LH, Webb LS, Peters LL, Hawes NL, Chang B, Zheng QY. Mouse models of USH1C and DFNB18: phenotypic and molecular analyses of two new spontaneous mutations of the USH1c gene. Hum. Mol. Genet 2003;12:3075–3086. [PubMed: 14519688]

Kato AS, Siuda ER, Nisenbaum ES, Bredt DS. AMPA receptor subunit-specific regulation by a distinct family of type II TARPs. Neuron 2008 2008;59(6):986–996.

Kremer H, van Wijk E, Märker T, Wolfrum U, Roepman R. Usher syndrome: molecular links of pathogenesis, proteins and pathways. Hum. Mol. Genet 2006;15:R262–R270. [PubMed: 16987892]

Lefevre G, Michel V, Weil D, Lepelletier L, Bizard E, Wolfrum U, Hardelin JP, Petit C. A core cochlear phenotype in USH1 mouse mutants implicates fibrous links of the hair bundle in its cohesion, orientation and differential growth. Development 2008;135:1427–1437. [PubMed: 18339676]

Letts VA, Felix R, Biddlecome GH, Arikkath J, Mahaffey CL, Valenzuela A, Bartlett FS 2nd, Mori Y, Campbell KP, Frankel WN. The mouse stargazer gene encodes a neuronal Ca2+channel gamma subunit. Nat. Genet 1998;19(4):340–347. [PubMed: 9697694]

Liu X, Udovichenko IP, Brown SD, Steel KP, Williams DS. Myosin VIIa participates in opsin transport through the photoreceptor cilium. J. Neurosci 1999;19:6267–6274. [PubMed: 10414956]

Lütcke A, Jansson S, Parton RG, Chavrier P, Valencia A, Huber L, Lehtonen E, Zerial M. Rab17, a novel small GTPase, is specific for epithelial cells and is induced during cell polarization. J. Cell Biol 1993;121(3):553–564. [PubMed: 8486736]

Maerker T, van Wijk E, Overlack N, Kersten FF, McGee J, Goldmann T, Sehn E, Roepman R, Walsh EJ, Kremer H, Wolfrum U. A novel Usher protein network at the periciliary reloading point between molecular transport machineries in vertebrate photoreceptor cells. Hum. Mol. Genet 2008;17:71–86. [PubMed: 17906286]

McGee J, Goodyear RJ, McMillan DR, Stauffer EA, Holt JR, Locke KG, Birch DG, Legan PK, White PC, Walsh EJ, Richardson GP. The very large G-protein-coupled receptor VLGR1: a component of the ankle link complex required for the normal development of auditory hair bundles. J. Neurosci 2006;26:6543–6553. [PubMed: 16775142]

Michalski N, Michel V, Bahloul A, Lefevre G, Barral J, Yagi H, Chardenoux S, Weil D, Martin P, Hardelin JP, Sato M, Petit C. Molecular characterization of the ankle-link complex in cochlear hair cells and its role in the hair bundle functioning. J. Neurosci 2007;27:6478–6488. [PubMed: 17567809]

Moser T, Brandt A, Lyskowski A. Hair cell ribbon synapses. Cell Tissue Res 2006;326:347–359. [PubMed: 16944206]

Neco P, Giner D, del Mar Frances M, Viniegra S, Gutierrez LM. Differential participation of actin- and tubulin-based vesicle transport systems during secretion in bovine chromaffin cells. Eur. J. Neurosci 2003;18:733–742. [PubMed: 12924999]

Payne HL. The role of transmembrane AMPA receptor regulatory proteins (TARPs) in neurotransmission and receptor trafficking (Review). Mol. Membr. Biol 2008;25(4):353–362. [PubMed: 18446621]

Pujol R. Morphology, synaptology and electrophysiology of the developing cochleae. Acta Otolaryngol 1985;421:5–9.

Pujol, R.; Lavigne-Rebillard, M.; Lenoir, M. Development of sensory and neural structures in the mammalian cochleae. New York: Springer; 1998.

Raphael Y, Altschuler RA. Structure and innervation of the cochlea. Brain Res. Bull 2003;60(5–6):397–422. [PubMed: 12787864]

Reiners J, Nagel-Wolfrum K, Jürgens K, Märker T, Wolfrum U. Molecular basis of human Usher syndrome: Deciphering the meshes of the Usher protein network provides insights into the pathomechanisms of the Usher disease. Exp. Eye Res 2006;83:97–119. [PubMed: 16545802]

Reiners J, Reidel B, El-Amraoui A, Boëda B, Huber I, Petit C, Wolfrum U. Differential distribution of harmonin isoforms and their possible role in Usher-1 protein complexes in mammalian photoreceptor cells. Invest. Ophthalmol. Vis. Sci 2003;44:5006–5015. [PubMed: 14578428]

Rivolta MN, Grix N, Lawlor P, Ashmore JF, Jagger DJ, Holley MC. Auditory hair cell precursors immortalized from the mammalian inner ear. Proc. R. Soc. Lond. B 1998;265:1595–1603.

Rivolta MN, Halsall A, Johnson CM, Tones MA, Holley MC. Transcript profiling of functionally related groups of genes during conditional differentiation of a mammalian cochlear hair cell line. Genome Res 2002;12:1091–1099. [PubMed: 12097346]

Roux I, Safieddine S, Nouvian R, Grati M, Simmier M, Bahloul A, Perfettini I, Le Gall M, Rostaing P, Hamard G, Triller A, Avan P, Moser T, Petit C. Otoferlin, defective in a human deafness form, is essential for exocytosis at the auditory ribbon synapse. Cell 2006;127:277–289. [PubMed: 17055430]

Ruel J, Wang J, Rebillard G, Eybalin M, Lloyd R, Pujol R, Puel JL. Physiology, pharmacology and plasticity at the inner hair cell synaptic complex. Hear. Res 2007;227(1–2):19–27. [PubMed: 17079104]

Siemens J, Kazmierczak P, Reynolds A, Sticker M, Littlewood-Evans A, Müller U. The Usher syndrome proteins cadherin 23 and harmonin form a complex by means of PDZ-domain interactions. PNAS 2002;99:14946–14951. [PubMed: 12407180]

Sterling P, Matthews G. Structure and function of ribbon synapses (Review). Trends Neurosci 2005;28 (1):20–29. [PubMed: 15626493]

Sobkowitz H, Rose J, Scott G, Slapnick S. Ribbon synapses in the developing intact and cultured organ of Corti in the mouse. J. Neurosci 1982;2(7):942–957. [PubMed: 7097321]

Tomita S, Shenoy A, Fukata Y, Nicoll RA, Bredt DS. Stargazin interacts functionally with the AMPA receptor glutamate-binding module. Neuropharmacology 2007;52(1):87–91. [PubMed: 16919685]

Trojan P, Krauss N, Choe HW, Giessl A, Pulvermüller A, Wolfrum U. Centrins in retinal photoreceptor cells: regulators in the connecting cilium. Prog. Retin. Eye. Res 2008;27(3):237–259. [PubMed: 18329314]

van Wijk E, van der Zwaag B, Peters T, Zimmermann U, Te Brinke H, Kersten FF, Märker T, Aller E, Hoefsloot LH, Cremers CW, Cremers FP, Wolfrum U, Knipper M, Roepman R, Kremer H. The DFNB31 gene product whirlin connects to the Usher protein network in the cochlea and retina by direct association with USH2A and VLGR1. Hum. Mol. Genet 2006;15(5):751–765. [PubMed: 16434480]

Velasco A, Hendricks L, Moremen KW, Tulsiani DR, Touster O, Farquhar MG. Cell type-dependent variations in the subcellular distribution of alpha-mannosidase I and II. J. Cell Biol 1993;122(1):39–51. [PubMed: 8314846]

Verpy E, Leibovici M, Zwaenepoel I, Liu XZ, Gal A, Salem N, Mansour A, Blanchard S, Kobayashi I, Keats BJ, Slim R, Petit C. A defect in harmonin, a PDZ domain-containing protein expressed in the inner ear sensory hair cells, underlies Usher syndrome type 1C. Nat. Genet 2000;26:51–55. [PubMed: 10973247]

Weil D, Blanchard S, Kaplan J, Guilford P, Gibson F, Walsh J, Mburu P, Varela A, Levilliers J, Weston MD, Kelley PM, Kimberling WJ, Wagenaar M, Levi-Acobas F, Larget-Piet D, Munnich A, Steel KP, Brown SDM, Petit C. Defective myosin VIIIA gene responsible for Usher syndrome type 1B. Nat. Genet 1995;374:60–61.

Weil D, El-Amraoui A, Masmoudi S, Mustapha M, Kikkawa Y, Lainé S, Delmaghani S, Adato A, Nadifi S, Zina ZB, Hamel C, Gal A, Ayadi H, Yonekawa H, Petit C. Usher syndrome type 1 G (USH1G) is caused by mutations in the gene encoding SANS, a protein that associates with the USH1C protein, harmonin. Hum. Mol. Genet 2003;12:463–471. [PubMed: 12588794]

Weston MD, Luijendijk MWJ, Humphrey KD, Möller C, Kimberling WJ. Mutations in the VLGR1 gene implicate G-protein signaling in the pathogenesis of Usher syndrome type II. Am. J. Hum. Genet 2004;74:357–366. [PubMed: 14740321]

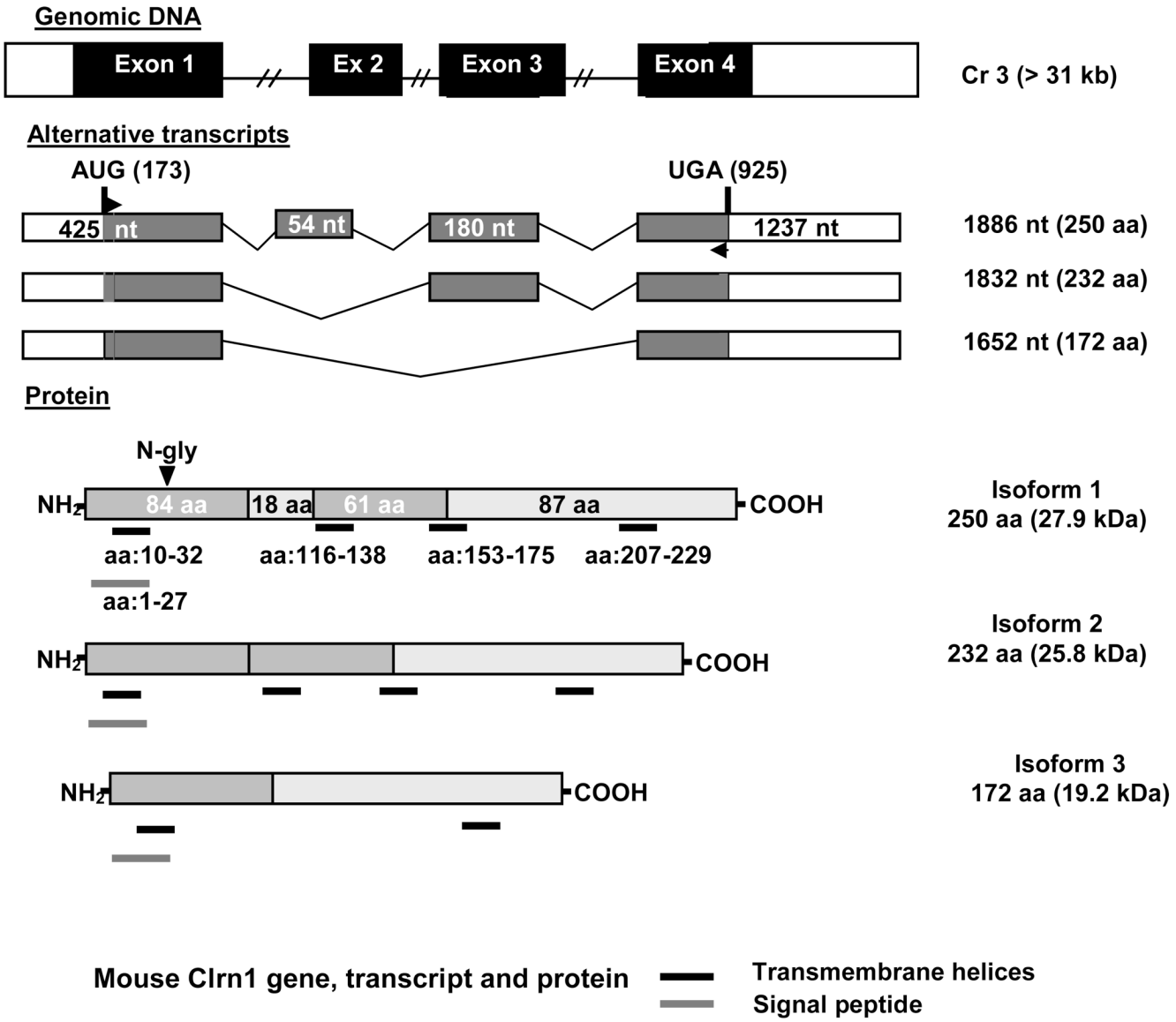

Figure 1.

Gene structure, transcripts, and protein isoforms of clarin-1. The structural gene encoding clarin-1 contains four exons that can be alternatively spliced to yield three putative transcripts. The three transcripts can be translated into three different protein isoforms. Isoforms 1 and 2 contain all four transmembrane domains, and are thus true tetraspanins. Alternative splicing removing exons 2 and 3 results in removal of two transmembrane domains, and thus isoform 3 is not a tetraspanin.

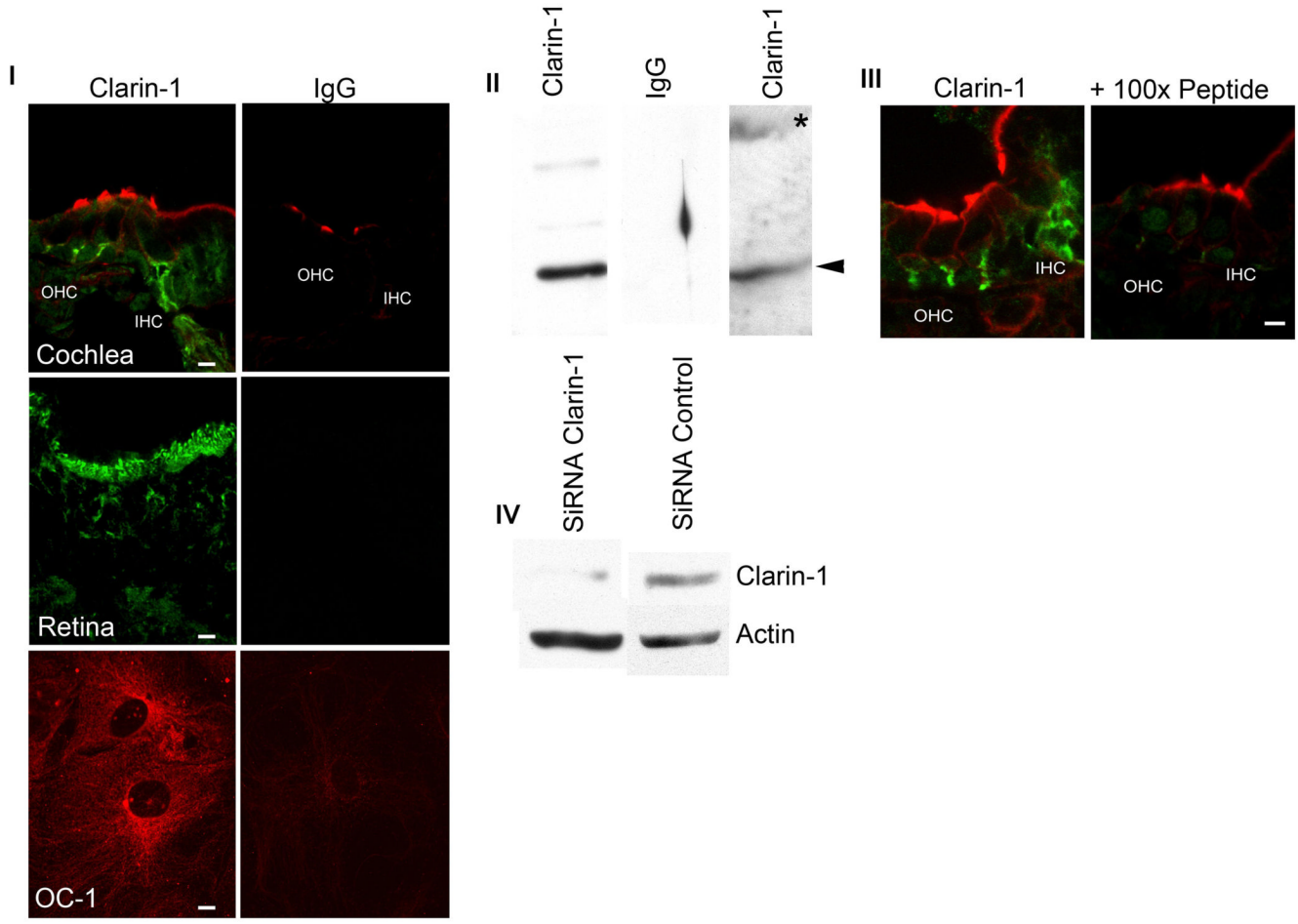

Figure 2.

Anti-clarin-1 antibody qualification. Panel I: P3 mid-modiolar cross sections, P28 eye and differentiated UB/OC-1 cells were incubated with anti-clarin-1 antibody or normal rabbit IgG and analyzed by fluorescence confocal microscopy (see Materials and Methods). Panel II: Western blot analysis of P3 cochlea (lane 1 and 2) and UB/OC-1 cells (lane 3) transfected with GFP-clarin-1 fusion protein. Membranes were probed with anti-clarin-1 antibody (lane 1 and 3) or normal rabbit IgG (lane 2). Arrowheads denote endogenous clarin-1. Asterisk denotes GFP-clarin-1 fusion protein. Panel III: Confocal microscopy of P3 mid-modiolar sections incubated with anti-clarin-1 antibody alone or in the presence of 100-fold molar excess the fusion protein used to generate the antibody. Panel IV: Western blot analysis of UB/OC-1 cells transfected with a siRNA specific for clarin-1 (lane 1) or an unrelated siRNA (lane 2). The membrane was cut in half and probed with either anti-clarin-1 or with anti-β-actin antibodies, as loading control (bottom).

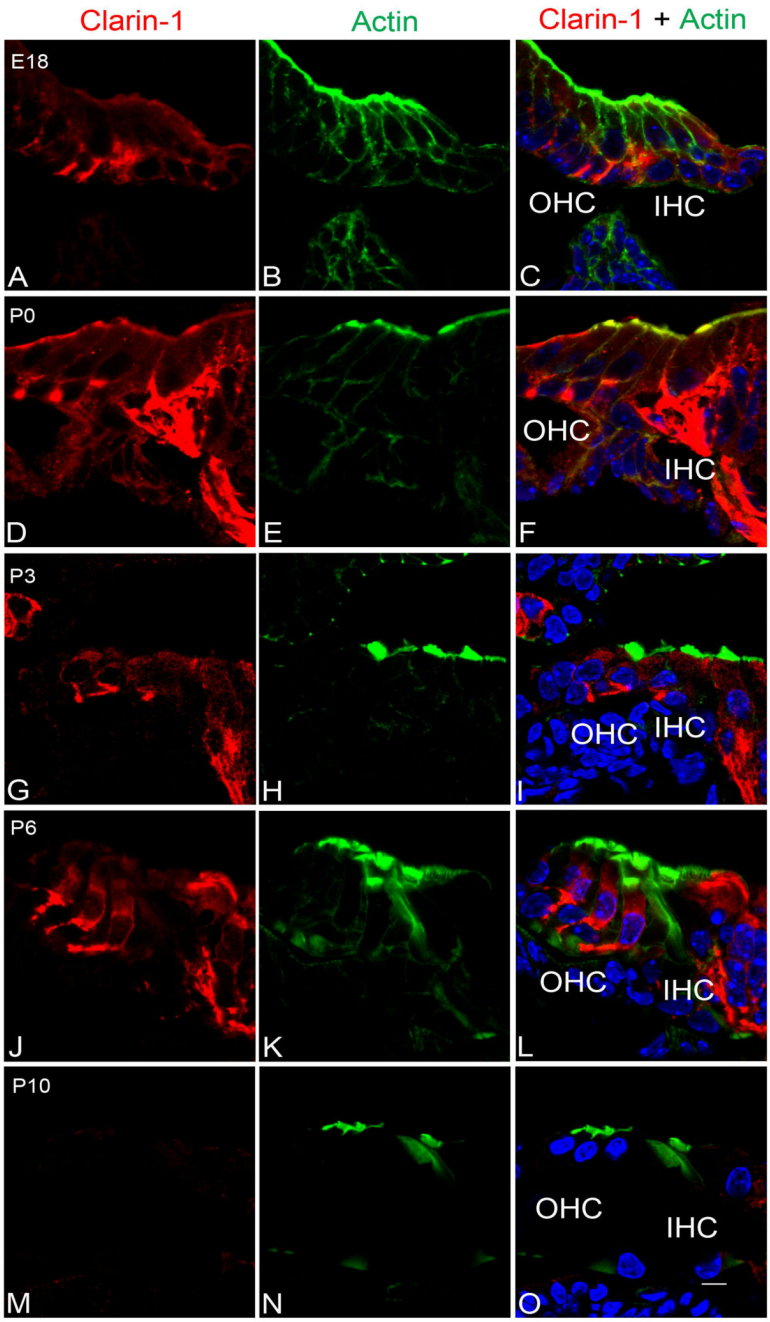

Figure 3.

Developmental expression of clarin-1 in the mouse cochleae. Cochleae were microdissected at the indicated ages. Sections were blocked for 30 min with 10% milk containing 0.2% Tween-20 and then incubated overnight with the first antibody anti-clarin-1 (red). After several washes the sections were incubated with the secondary antibody and phalloidin (green) for 1 h and mounted using Vectashield mounting media with DAPI. **A–C**: E18 cochleae, **D–F**: P0 cochleae, **G–I**: P3 cochleae, **J–L**: P6 cochleae, **M–O**: P10 cochleae. **A, D, G, J, M**: clarin-1; **B, E, H, K, N**: phalloidin; **C, F, I, L, O**: merge images. IHC: inner hair cells. OHC: outer hair cells. Scale bar: 5 μm.

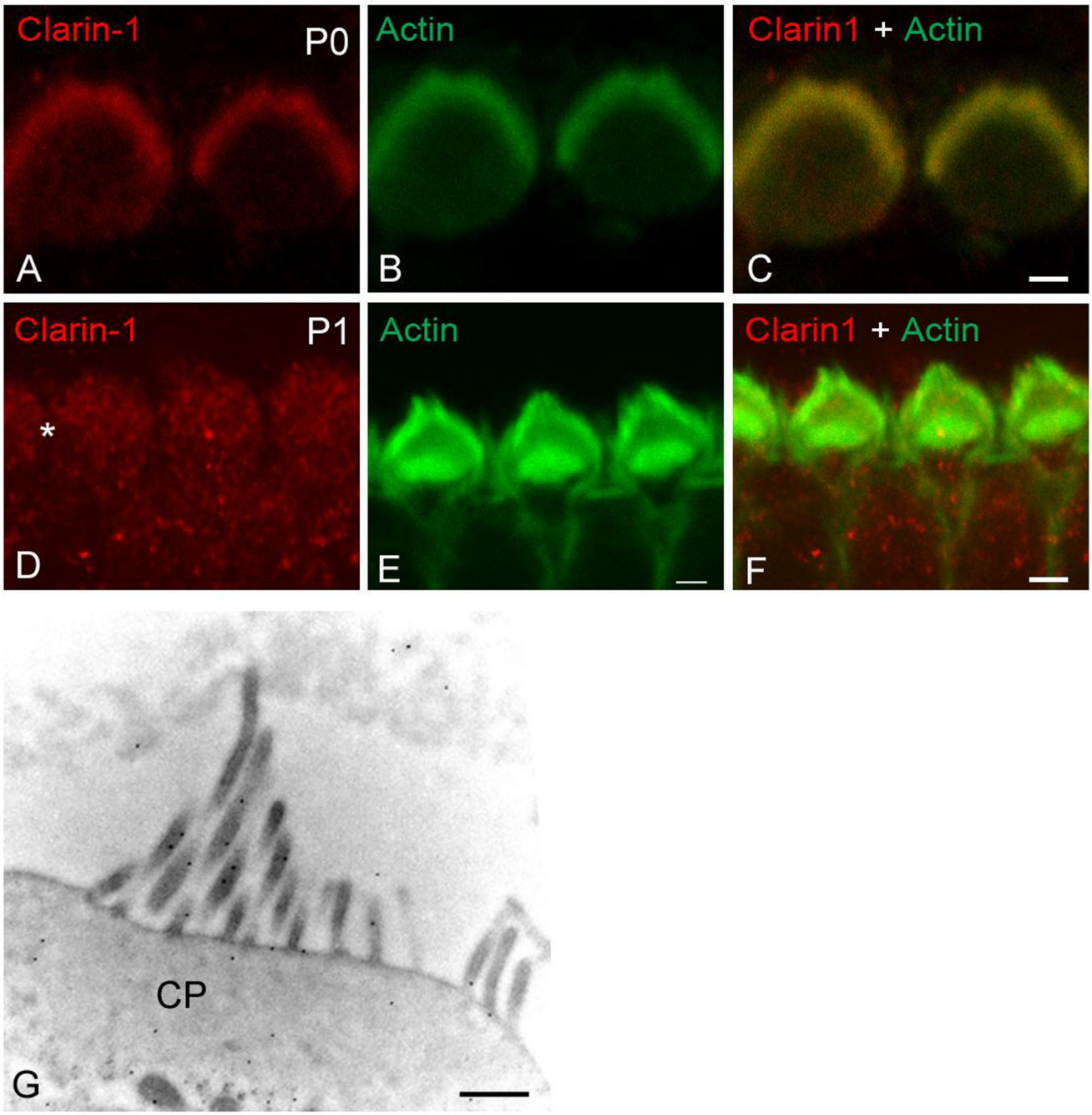

Figure 4.

Expression of clarin-1 at the apical aspect of hair cells. Surface preparations of P0 (A–C) and P1 (D–F) organs of Corti were analyzed by confocal microscopy. A, D: immunostained for clarin-1. B, E: counterstained with phalloidin. C, F: merge image. Asterisk denotes weak immunostaining for clarin-1 in the cell bodies. G: Immunogold localization of clarin-1 in outer hair cells from P0 mice. Ultrastructural localization is consistent with low resolution localization shown in Figure 3. CP: cuticular plate. Scale bar: A–C: 1 μm, D–F: 2 μm, G: 500 nm.

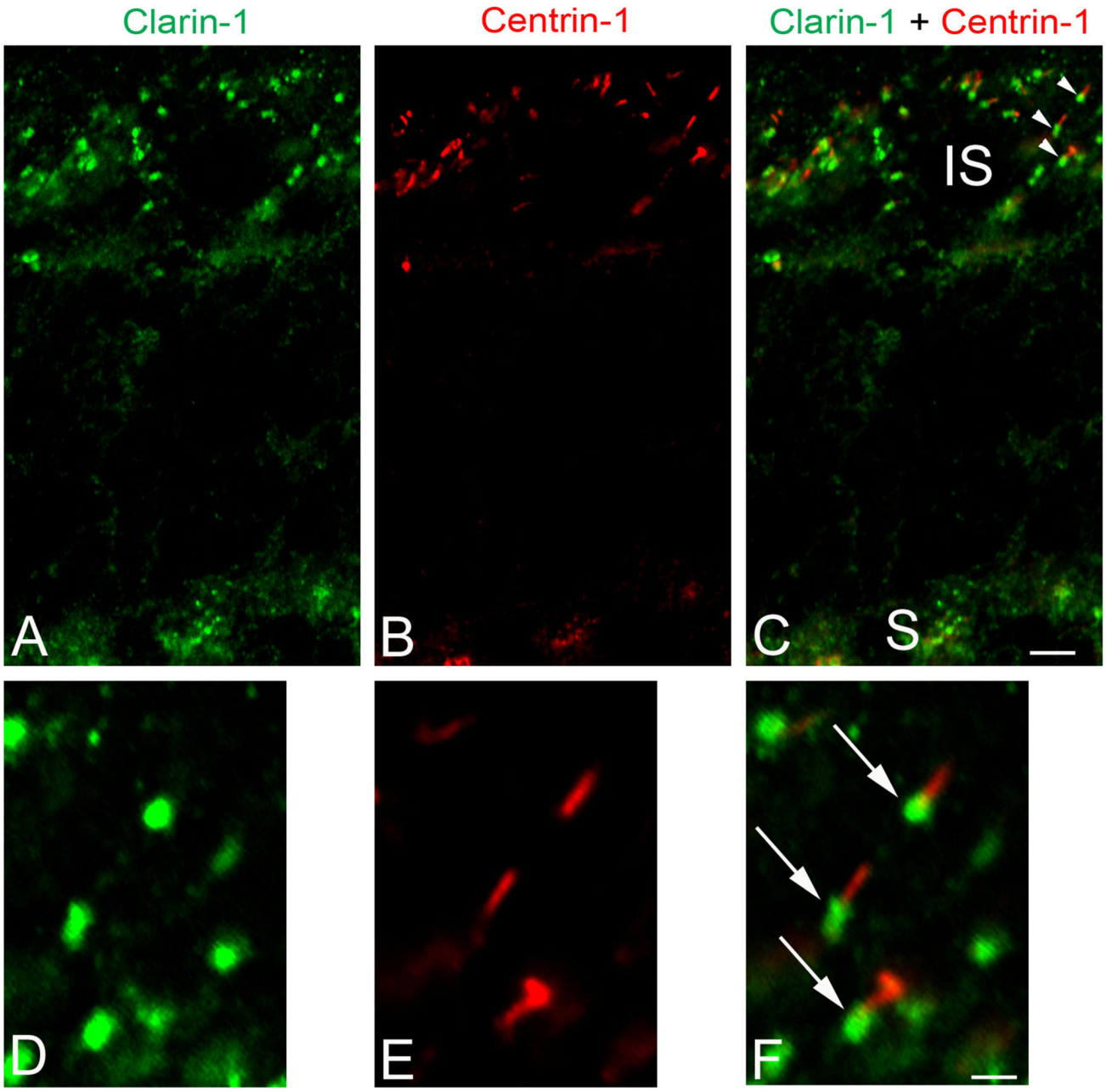

Figure 5.

Dual-immunofluorescence analysis of clarin-1 and centrin-1 in acetone fixed retina from P28 wild type mouse. **A–C**: Whole retina showing immunostaining for clarin-1 (A) in the inner segments of photoreceptors cells (IS), connecting cilia (shown by colocalization with centrin-1, **C**) and ribbon synapses (S). **D–F**: A higher magnification of an area of figures A–C (see arrowheads) demonstrating expression of clarin-1 only at the basal aspect of the connecting cilia (arrows) shown by partial colocalization with centrin-1. **A, D**: immunostaining for clarin-1; **B, E**: immunostaining for centrin-1; **C, F**: merge images. Scale bar: 5 μm (**A–C**), 1 μm (**DF**).

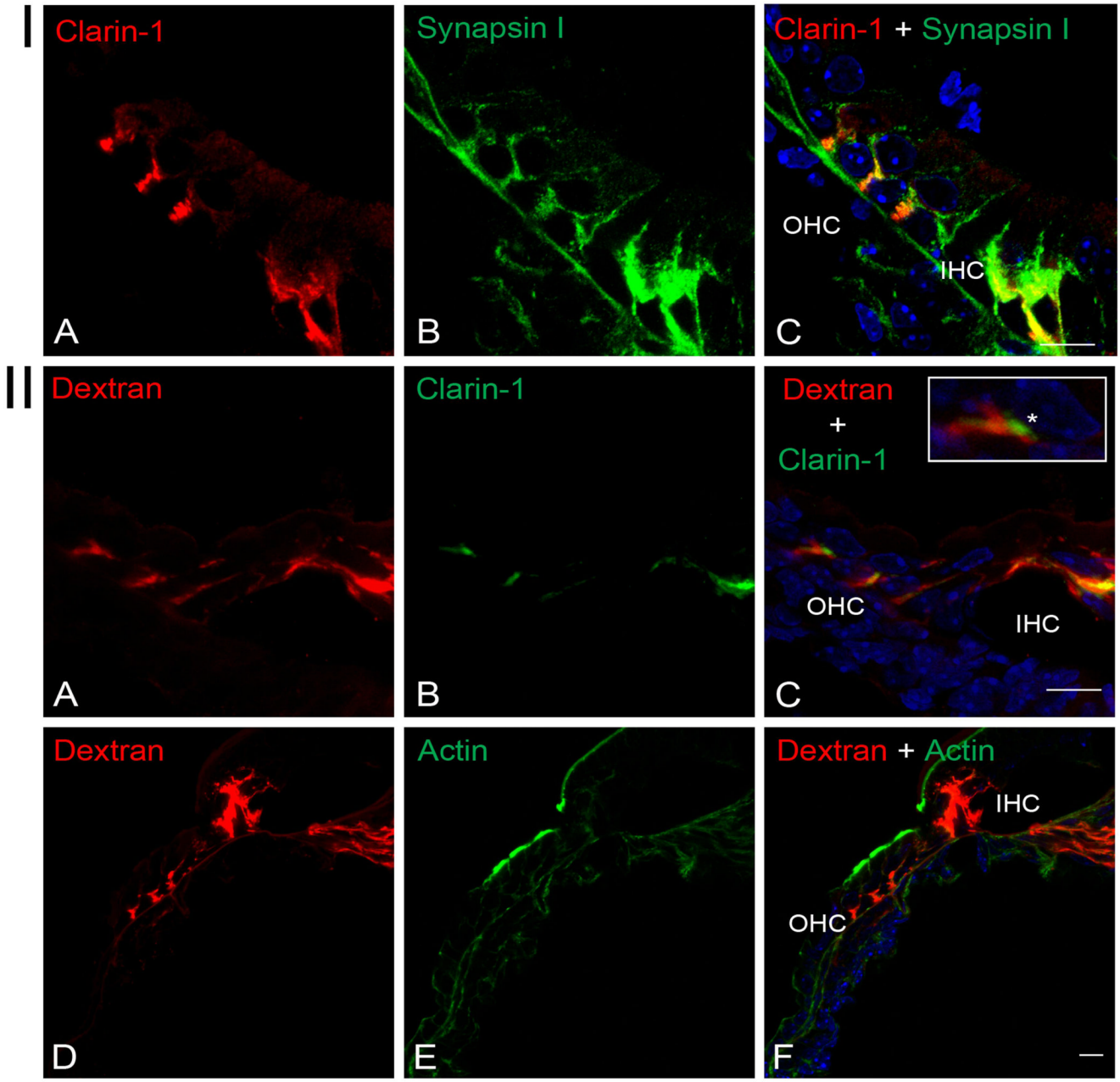

Figure 6.

Localization of clarin-1 to the type I afferent terminals in P3 mouse cochleae. **Panel I**: Dual immunostaining of clarin-1 and synapsin-I showing colocalization at the end of the synaptic terminals below the OHCs and at the base of the IHC. **Panel II**: Clarin-1 is expressed in type I afferent terminals. **A–C**: P3 cochleae were labeled with a neuronal tracer (**A**) (Huang et al. 2007) and immunostained with anti-clarin-1 antibody (**B**). Inset shows presynaptic expression of clarin-1 (asterisk) in an outer hair cell, determined for the absence of dextran staining. **D–F**: Counterstained with the fluorochrome-conjugated dextran (**D**) and phalloidin (**E**), to show integrity of the organ of Corti. OHC: outer hair cells. IHC: inner hair cells. Scale bar: 10 μm.

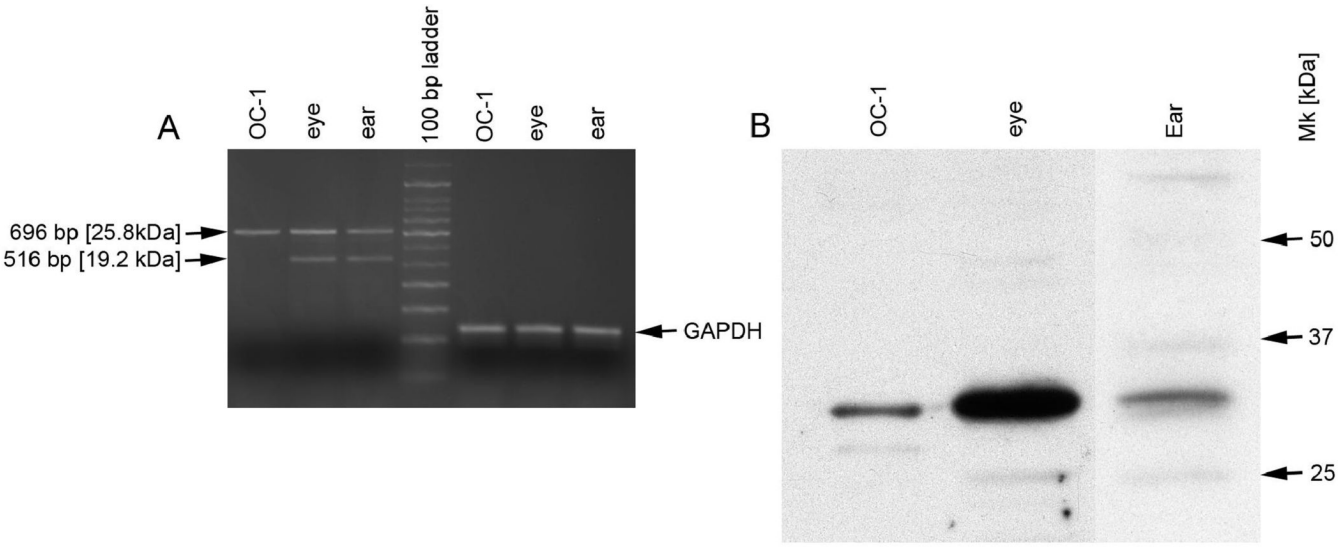

Figure 7.

Expression of clarin-1 isoforms in eye, ear, and differentiated UB/OC-1 cells. **A**: Total RNA was isolated from newborn mouse cochlea (ear), whole eyes from 4 week old mice (eye) or differentiated UB/OC-1 cells and analyzed by RT-PCR for clarin-1 mRNA using primers flanking the coding region in exon 1 (forward primer) and 4 (reverse primer). GAPDH mRNA (a housekeeping gene) was analyzed as a control for loading. Note that the transcripts encoding isoforms 2 and 3 of clarin-1 are present in both cochlea and eye, while only the transcript for isoform 2 is present in UB/OC-1 cells. **B**: Western blot analysis of clarin-1 protein in retina (4 week old mice), cochlea (P0 ice) and differentiated UB/OC-1 cell extracts. A single isoform of clarin-1 is predominantly expressed in all 3 samples which must be isoforrm 2 based on the clarin-1 mRNA results, suggesting isoform 2 is the predominant functional isoform in photoreceptors and hair cells.

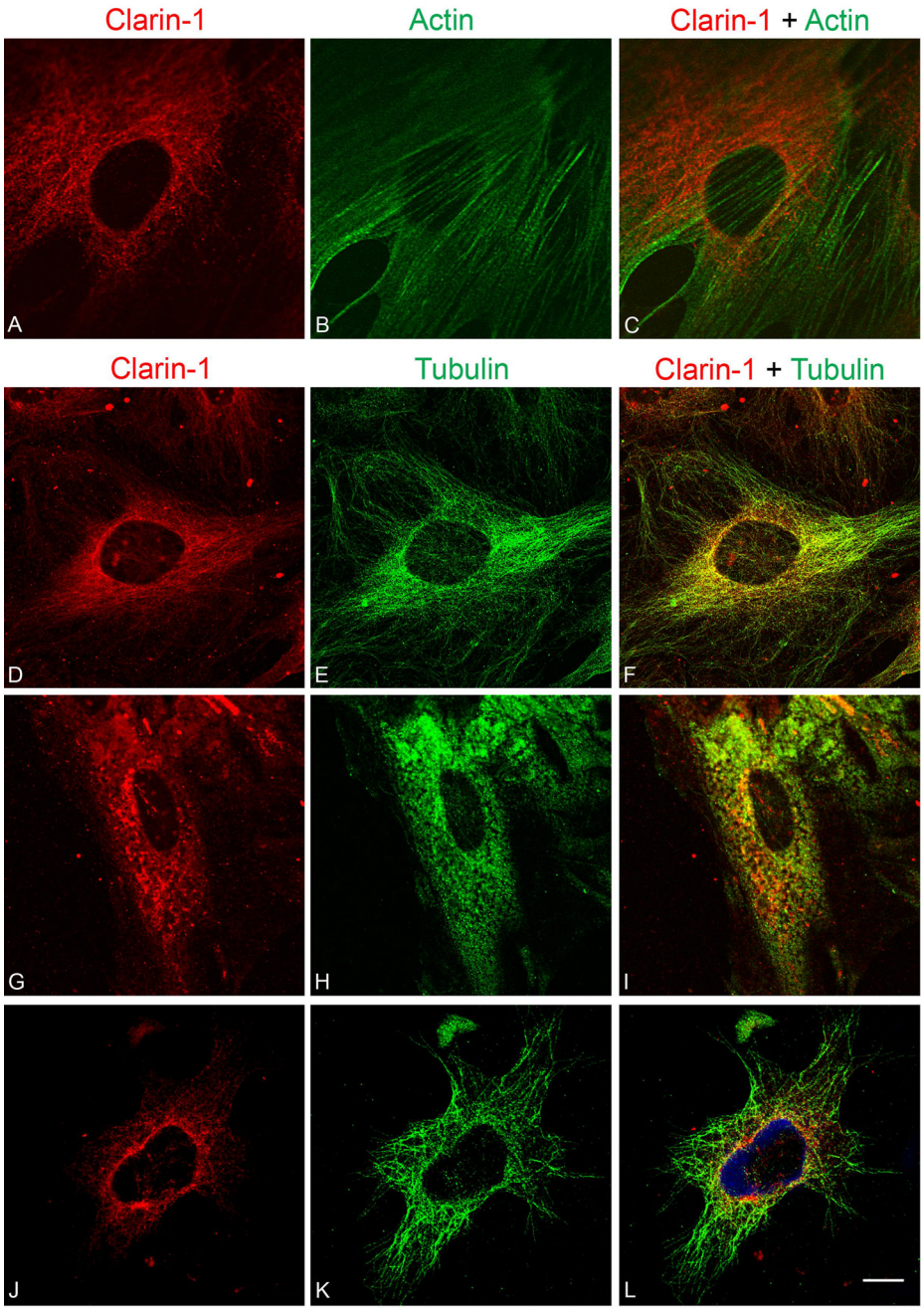

Figure 8.

Immunofluorescence analysis of clarin-1 in differentiated UB/OC-1 cells. **A, D, G, J**: UB/OC-1 cells were immunostained using affinity purified anti-clarin-1 antibody (red). **B**: Phalloidin counterstain (green) demonstrates that clarin-1 does not colocalize with actin filaments (**C**). **E**: Immunostaining with tubulin (green) shows colocalization of clarin-1 with microtubules (**F**). **G–I**: Treatment with nocodazole (10 μM), abolishes filamentous localization of both tubulin (**H**) and clarin-1 (**G**). **J–L**: Tyrphostin A8 (20 μM), which disrupts post-trans Golgi vesicle trafficking, affects only clarin-1 distribution. **C, F, I, L**: Merge images. Scale bar: 20 μm.

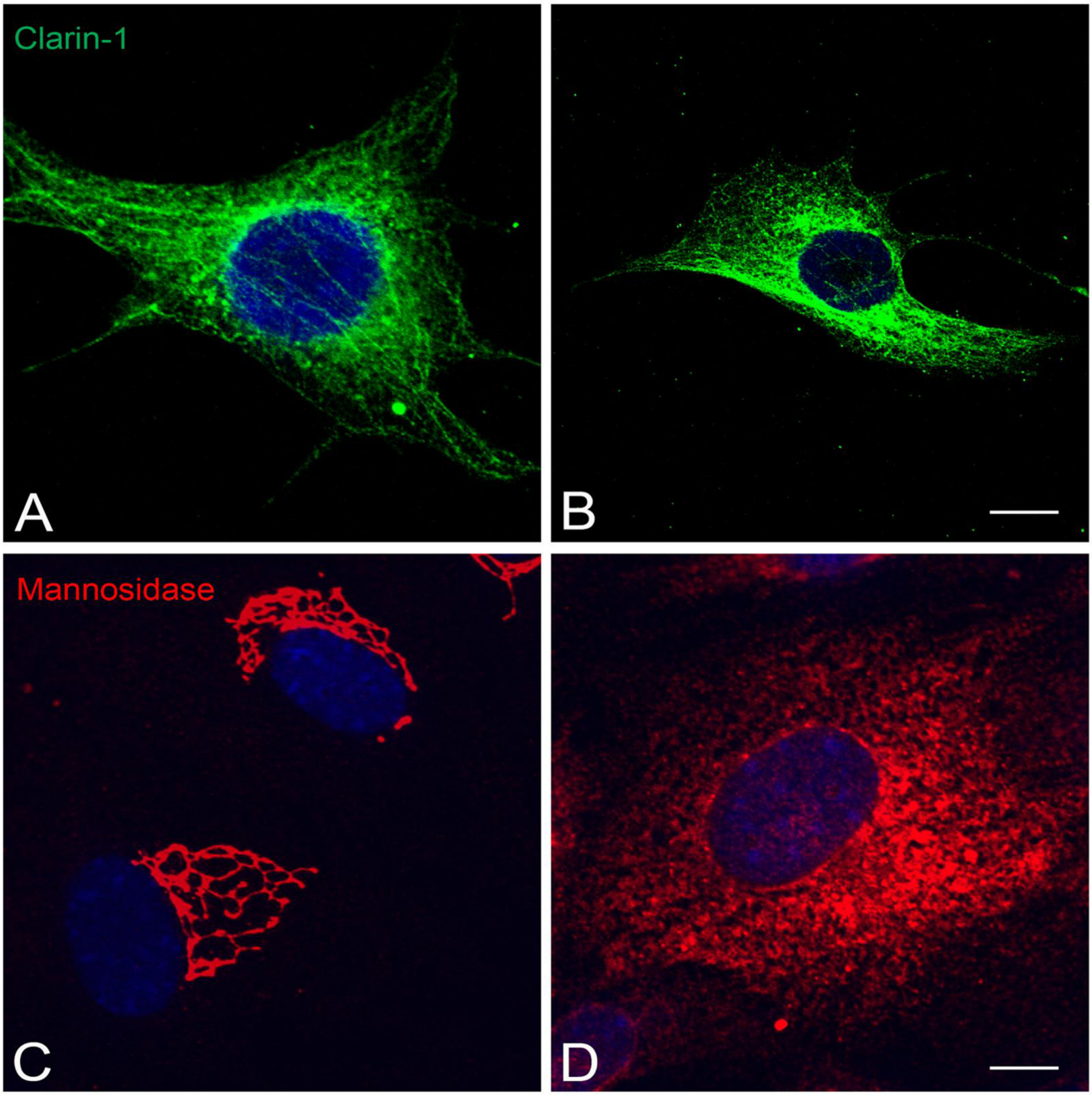

Figure 9.

Immunofluorescence analysis of clarin-1 in differentiated UB/OC-1 cells treated with brefeldin A. **A, B**: Immunostaining with clarin-1 antibody in cells incubated with vehicle alone (**A**) or with 1 μg/ml of brefeldin A (**B**). **C, D**: UB/OC-1 cells immunostained with anti-Mannosidase II antibody in the absence (**C**) or presence (**D**) of brefeldin A. There is no effect on clarin-1 distribution upon treatment with brefeldin A while Mannosidase II shifted from a very specific medial Golgi distribution to a scattered intracellular pattern after 30 minutes incubation with the drug. Scale bar: 20 μm.